CONFERENCE PRE-PRINT

HOW "THE TAIL WAGS THE DOG": PHYSICS OF EDGE-CORE COUPLING BY INWARD TURBULENCE PROPAGATION

Mingyun Cao
Department of Physics and Astronomy, University of California, Los Angeles
Los Angeles, the United States
Email: mcao@physics.ucla.edu

P.H. Diamond
Departments of Physics and Astronomy & Astrophysics, University of California, San Diego
La Jolla, the United States

Abstract

The dynamics of edge-core coupling is critically important to the optimal performance of magnetically confined fusion plasmas. Since early proposals, there has been persistent speculation that inward propagation of turbulence from the boundary is a possible means to energize the edge-core coupling region. However, the detailed mechanism of this process has remained a mystery until recent experiments observed that regular, intense gradient relaxation events generated blob-void pairs very close to the last closed flux surface. Blobs ($\tilde{n} > 0$) propagate outward into the scrape-off layer (SOL), while voids ($\tilde{n} < 0$) propagate inward, and so stir the core plasma. Here, we demonstrate that this heretofore ignored process of void emission can drive a broad turbulent layer of width $\sim 100\,\rho_s$, for typical parameters. The mechanism is the Cherenkov emission of drift waves from inward-propagating voids. The model shows promise to resolve several questions surrounding the shortfall problem and the strong turbulence in the edge-core coupling region.

1. INTRODUCTION

Turbulence is often thought of as a multi-ingredient concoction—a "soup" containing eddys, waves, structures, etc. Here, "structures" may refer to vortices, density blobs, phase space holes, etc. [1–5]. Structures are distinguished from ordinary eddys by extended lifetimes and a self-binding character that maintains them against stochastic shear stresses. The well-known and physically appealing Okubo-Weiss criterion gives one measure of the resilience of a vortex structure [6,7]. In magnetically confined fusion plasmas, structures are present in the form of blobs and voids that are plasma filaments with large-amplitude positive or negative density fluctuations. Blobs and voids propagate in opposite directions, down and up the mean gradient, respectively [8,9]. As voids move inward and thus stay in the bulk plasma, they can be viewed as messengers sent from the edge to the core.

This inward motion of voids brings us to the dynamics of edge-core coupling, which is critical to the optimization of magnetically confined fusion plasmas [10]. To this end, the physics of what sets the width of the edge-core coupling region, where the turbulence level sometimes exceeds the prediction of standard Fickian gyrokinetic models, has long been a "known unknown". This is referred to as the "shortfall problem" [11,12]. The edge-core coupling region is also named as "no man's land" (NML) because it falls between the domains of the conventional core and edge models and codes [5]. Since early proposals by B.B. Kadomtsev [13], there has been persistent speculation that inward propagation of turbulence from the boundary is a means to energize the NML [14]. However, no work has set forth a detailed physical picture that explains how "the tail (edge) wags the dog (core)". No reasonable estimates of the inward turbulence intensity flux and the width of the NML have been proposed, either.

Recent beam emission spectroscopy (BES) studies confirmed that, in L-mode, regular, intense gradient relaxation events (GREs) generated blob-void pairs very close to the last closed flux surface (LCFS) in tokamaks [15]. Thus, GREs pervade plasma boundary turbulence with coherent structures. In particular, blobs propagate outward into the scrape-off layer (SOL), while voids propagate inward and so stir the NML. Recently, it has been found that the shortfall is resolved in flux-driven gyrokinetic simulations, where relaxation of mean gradients is allowed [16]. This suggests a correlation between GREs and the formation of NML. As a concrete entity produced from GREs and delivered from edge to core, a void is a promising mediator of the inward turbulence spreading. On MAST, experiments show that the detection of a void is usually followed by a burst in zonal flow power [17]. A similar phenomenon is also observed in the latest experimental results from the stellarator TJ-K. This is direct evidence that coherent structures can drive zonal flow and play an important role in plasma turbulence dynamics.

Existing studies on coherent structures primarily focus on the scaling of their convection velocity in different plasma regimes. Although the interaction between drift waves and zonal flows has been well established, the interaction of coherent structures, another important component of plasma turbulence, with the former two has rarely been discussed. Therefore, current research on coherent structures is insufficient to account for the above results. Another regrettable fact is that far more attention has been given to blobs than to voids. In other words, there are millions of papers on blobs, while the scale of papers on voids is far less in comparison. This is likely attributed to the challenges in diagnosing voids—since they move inward, it is not feasible to insert probes too deeply into the plasma. To resolve the shortfall problem and figure out the role that voids play in inward turbulence spreading, we need a model that treats voids on an equal footing with drift waves and zonal flows.

Here, by developing a first-principles model incorporating density voids into turbulence dynamics, we demonstrate that the Cherenkov emission of drift waves from inward-moving voids generated at the edge drives substantial inward turbulence spreading. The physical picture of our model can be illustrated by the cartoon in Fig. 1. After being generated from GREs at ψ_0, inward-moving voids (deep blue circles) will excite a "radiation field," which can be divided into a near field and a far field. In the near field, the void drives an interchange response, which converts to a drift wave turbulence (light blue shades) in the far field. While voids "evaporate" at ψ_1, void-induced turbulence can propagate deeper and energize the NML in the range from ψ_2 to ψ_1. This turbulence is regulated by self-generated zonal flow, originating due to radiation-driven Reynolds stress. Concomitantly, the (ambient) turbulence and zonal flow can smear or shear the void, thereby constraining its lifetime, and so regulating turbulence production. For typical parameters, our theory predicts the following:

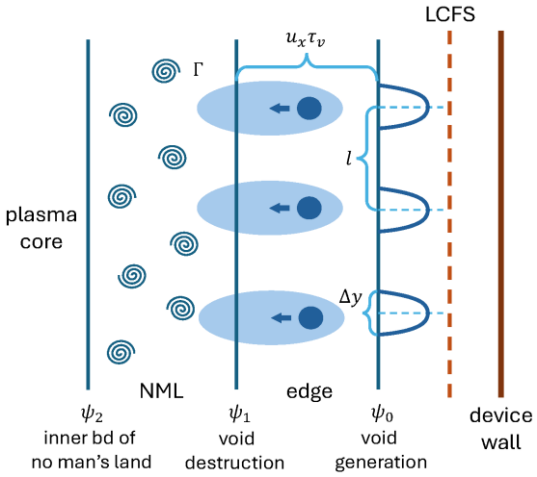

FIG. 1 Illustration of the energization of the no man's land by inward-moving voids. The confined plasma core is to the left of the magnetic surface ψ_2. The wall of the device is to the right of the LCFS.

(a) The width of the NML, which is determined by ratio of the void-induced turbulence spreading and the local production, and thus depends on the void parameters, is of order $100\,\rho_s$.
(b) The shearing rate of the void-driven zonal flow is comparable to or even exceeds the ambient shear.
(c) The void lifetime ranges from a few to $100\,\mu s$, which encompasses the observed experimental values reasonably well.

2. MODEL DEVELOPMENT

When developing a new model from scratch, it is always valuable to draw inspiration from "golden oldies." Recall that an accelerating charged particle radiates electromagnetic waves [18]. In the context of plasma physics, another example is that a moving screened plasma test particle (macro particle) radiates plasma waves [19]. Similarly, if we think of a void as a macro particle, it is natural to consider that it would also emit waves while moving through the background plasma. The next question relates to what kind of waves the moving void emits. One way to address this is to identify which dynamical processes are relevant at the spatiotemporal scales of the voids. Experimental results indicate that the radial propagation speed of voids is comparable to the electron diamagnetic drift velocity v_* [20,21]. This suggests that a moving void can excite drift waves, which motivates us to start from Hasegawa-Wakatani equation, the simplest model for drift waves [22].

2.1. Formulation of model based on Hasegawa-Wakatani model

Equation (1) is the Hasegawa-Wakatani equation with the curvature drive,

$$\begin{aligned} \frac{d}{dt}\nabla_\perp^2\varphi + 2\kappa\frac{1}{n_0}\frac{\partial n}{\partial y} &= D_\parallel\nabla_\parallel^2\left(\varphi - \frac{n}{n_0}\right) \\ \frac{1}{n_0}\frac{d}{dt}n &= D_\parallel\nabla_\parallel^2\left(\varphi - \frac{n}{n_0}\right) \end{aligned} \tag{1}$$

where

$$\frac{d}{dt}=\frac{\partial}{\partial t}+\boldsymbol{v}_{E\times\boldsymbol{B}}\cdot\nabla, D_{\parallel}=\frac{v_{\mathrm{the}}^2}{\nu_{ee}}\frac{1}{\rho_s^2\omega_{ci}}, n=n_0+\tilde{n}. \tag{2}$$

For simplicity, electrostatic potential φ, spatial and temporal coordinates, and velocities are nondimensionalized by T_e/e, ion sound speed gyroradius ρ_s, ion gyrofrequency ω_{ci}, and sound speed c_s, respectively. Here n is the plasma density, n_0 is the mean plasma density, $\kappa=\rho_s/R_c$ is the dimensionless magnetic curvature (R_c is the curvature radius of the magnetic field), v_{the} is the electron thermal velocity, and ν_{ee} is the electron-electron collision rate. To be compatible with the presence of drift waves, the adiabatic limit ($\alpha=D_{\parallel}k_{\parallel}^2/\omega>1$) should hold in regions away from the void. Here $k_{\parallel}$ and ω are the wave vector in the direction parallel to the magnetic field and the frequency of the drift wave. In the region near the void, however, adiabatic electrons are unfavourable, as they prohibit density mixing, which is indispensable to coherent structure formation. This implies that the hydrodynamic limit ($\alpha<1$) is relevant in the vicinity of the void, instead. Therefore, as illustrated in Fig. 2, the space of concern should be partitioned into two regimes: the near field regime where $\alpha<1$ and the far field regime where $\alpha>1$. By taking the corresponding limits, Eq. (1) reduces to

$$\begin{aligned}\frac{d}{dt}\nabla_{\perp}^2\varphi+2\kappa\frac{1}{n_0}\frac{\partial n}{\partial y}=0,\\ \frac{1}{n_0}\frac{d}{dt}n=0\end{aligned} \tag{3}$$

in the near field regime and

$$\frac{d}{dt}(\nabla_{\perp}^2\varphi-\varphi)-v_*\frac{\partial\varphi}{\partial y}=\frac{1}{n_0}\frac{dn_v}{dt} \tag{4}$$

in the far field regime, respectively. Note that Eq. (3) is identical to the classical two-field model (without dissipation) used to study self-propelled convection of coherent structures [23–25]. At the same time, the lhs of Eq. (4) is exactly the Hasegawa-Mima (HM) equation [26]. Voids enter the model via profile modulation, i.e., $n=n_0+n_v+\tilde{n}$, where n_v is the void density. Akin to test particle model [27], for tractability, we employ the delta-function-shaped expression for the void,

$$\frac{n_v}{n_0}=2\pi h\Delta x\Delta y\delta(x+u_xt)\delta\big(y-u_yt\big)H(t)H(\tau_v-t), \tag{5}$$

where $h=|n_v|/n_0\in(0.1,1)$ is the void magnitude, u_x and u_y are its radial and poloidal propagation speed. The spatial extent of the void Δx and Δy appear as the weight of the delta function. In addition, a product of two Heaviside step functions is introduced to account for the finite void lifetime τ_v. Throughout the rest of the letter, we focus primarily on the far field region, where turbulence excited by voids ultimately resides.

Treating the rhs of Eq. (4) as the source, we can solve the potential φ of the far field using the Green's function of the (linearized) HM equation. This approach follows that used in the dressed test particle model. See Appendix A for a detailed discussion on the linearization of Eq. (4). From this solution, we can further calculate the velocity field ($\tilde{\boldsymbol{v}}=\hat{\boldsymbol{z}}\times\nabla\varphi$) and the inward turbulence intensity flux Γ_I, yielding an evaluation of void-induced spreading and the extent of the NML. The Reynolds stress ($\langle\tilde{v}_x\tilde{v}_y\rangle$) and the shearing rate of void-driven zonal flow ($\omega_s^v=-\int\partial_x^2\langle\tilde{v}_x\tilde{v}_y\rangle\,dt$) can also be calculated. These allow for a direct comparison between ω_s^v and the ambient shear ω_s^a.

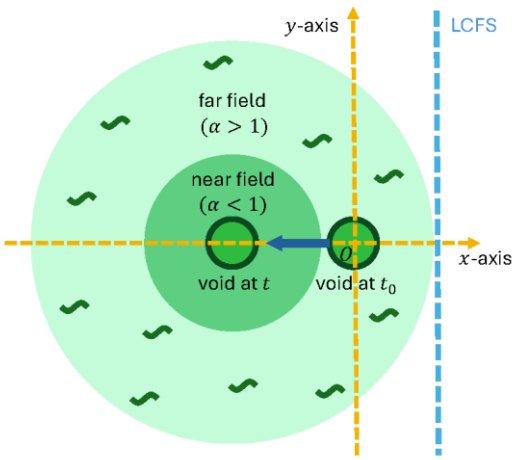

FIG. 2 The space of concern in our model can be divided into two regimes: the near field regime near the void ($\alpha<1$) and the far field regime away from the void ($\alpha>1$).

2.2. Green's function of the linearized Hasegawa-Wakatani model

Given the significance of the HM equation in plasma theory, surprisingly little literature exists on its Green's function. Fortunately, the Green's function of the linearized Rossby waves equation with a finite Rossby deformation radius, which is homotopic to the linearized HM equation, has been calculated in geophysics [28,29]. Thus the Green's function of the linearized HM equation is

$$G(\boldsymbol{r},t;\boldsymbol{r}',t') = -\int_{c-i\infty}^{c+i\infty} \frac{ds}{2\pi i} \exp\left(s\tau + \frac{v_* \chi}{2s}\right) \times \frac{1}{2\pi s} \mathrm{K}_0 \left[\left(1+\left(\frac{v_*}{2s}\right)^2\right)^{\frac{1}{2}} \rho\right], \tag{6}$$

where

$$\xi = x - x', \chi = y - y', \tau = t - t', \rho = |r - r'|, \tag{7}$$

and K_0 is the modified Bessel function of the second kind. As Eq. (6) is in integral form, a direct implementation of it is impractical. If we focus on the dynamics after the destruction of the void, we can utilize the asymptotic form of the Green's function in the limit of $\tau \to \infty$,

$$G \to -\frac{1}{2\pi}\frac{1}{\sqrt{v_* \rho \tau}} \cos\left[\sqrt{2v_*(\rho - \chi)\tau}\right] \text{ as } \tau \to \infty. \tag{8}$$

2.3. Local solutions of three limiting cases

Even so, this expression is still too complex for analytical computation. And the fact that the motion of the void has both radial and poloidal components makes solving the far field equation even more challenging. To gain physical insight, we decide to seek only the local solution for cases where the void moves purely in the radial or the poloidal direction. As labelled in Fig. 3, the three specific cases we consider and their spatial orderings are, for (a), a void moving in the radial direction ($u_y = 0$): (1) the solution away from the x axis but near the y axis, ($x \lesssim x' \sim u_x \tau_h \sim \Delta x \sim \Delta y \ll y$) and (2) the solution near the x axis but away from the y axis, ($y \lesssim x' \sim u_x \tau_h \sim \Delta x \sim \Delta y \ll x$); and for (b), a void moving in the poloidal direction ($u_x = 0$): (3) the solution away from the x axis but near the y axis, ($x \lesssim y' \sim u_y \tau_v \sim \Delta x \sim \Delta y \ll y$).

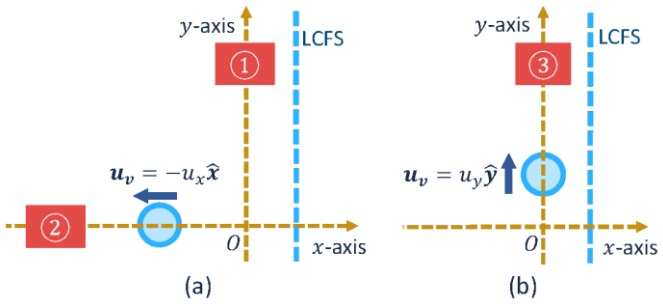

FIG. 3 Schematic of the specific cases we examine in this work: (a) void moves purely in the radial direction; (b) void moves purely in the poloidal direction.

Here, $x = 0$ refers to the birth zone of the void, and $y = 0$ can be thought of as the midplane. All three cases share the same temporal ordering,

$$1/\omega_* \ll t' \sim \tau_v \ll t. \tag{9}$$

Note that in each case, we have $\rho < v_* \tau$ to maintain causality. And as supported by experimental results [20], we also take $u_x, u_y \lesssim v_*$ so that the perturbation excited by voids could propagate ahead of the void.

3. QUANTITATIVE RESULTS

With the computed local solutions, we are now able to estimate the width of the no man's land and the shearing rate of the zonal flow driven by the voids.

3.1. Estimate of the no man's land width

The far field solution φ we calculate is effectively the turbulence field excited by voids and responsible for the void-induced inward spreading. As shown in Fig. 1, compared with the penetration depth of voids, the effects of the turbulence they excite could extend deeper into the main plasma ($\sim \psi_2$), and enhance the turbulence level in the turbulence level in the NML. The balance equation for the turbulence intensity (without dissipation) is

$$\frac{\partial}{\partial t}\langle \tilde{v}^2 \rangle = -\frac{\partial}{\partial x}\langle \bar{\Gamma}_I \rangle + \kappa \langle \tilde{v}\tilde{n} \rangle. \tag{10}$$

On the rhs, $\langle \Gamma_I \rangle$ is the turbulence intensity flux after poloidal and time averaging, and second term represents the local turbulence production rate. By integrating over the NML spanning from ψ_2 to ψ_1, we define the turbulence production ratio of turbulence spreading into the NML to overall local production in the NML as:

$$R_a = \langle \bar{\Gamma}_I \rangle|_{\psi_1} / \kappa \int_{\psi_2}^{\psi_1} \langle \tilde{v}\tilde{n} \rangle dr. \tag{11}$$

Here, $\langle \bar{\Gamma}_I \rangle|_{\psi_2}$ is neglected, as $x = \psi_2$ can be thought of as the cutoff line of voids' influence.

Our model provides us with an approximation of Γ_I. As illustrated in Fig. 1, the gradient relaxation events, or, the edge instabilities, contain N troughs in the poloidal direction, each of which can be considered as a void emitter. The spacing between individual emitters is denoted by l, and the width of the emitter is assumed to be of the order Δy, the characteristic size of voids. After each waiting time τ_w, N voids are emitted simultaneously. If each individual void contributes a pulse with a magnitude ΔI, a duration of τ_v, and a poloidal extent of Δy, then the total turbulence intensity flux can be estimated by the superposition of these pulses, i.e.,

$$\Gamma_I \sim \sum_{i,j} u_x \Delta I 2\pi \Delta y \tau_v \delta(y - il)\delta(t - j\tau_w), \tag{12}$$

where the indices i and j represent voids generated at different locations and times, respectively. Here we adopt u_x as the propagating speed of these pulses. We can think of this process as bulldozers (voids) pushing soil (turbulence pulses) at a speed of u_x. The magnitude ΔI can be obtained from the local solution at $x \to \psi_1^-$ in region 2 of Fig. 3. Consequently, the ratio given in Eq. (11) can be rewritten into

$$R_a = \left(\frac{h\Delta x \Delta y}{u_x \tau_v}\right)^2 \frac{2\pi}{v_* \tau_v^2} \frac{\Delta y}{a} \frac{\tau_v}{\tau_w} / (\kappa \langle \tilde{v}\tilde{n} \rangle w_{nml}) \tag{13}$$

where a is the minor radius of a tokamak. Here we consider a strong ballooning scenario ($N \sim \mathcal{O}(1)$) and approximate the local turbulence production as $\kappa \langle \tilde{v}\tilde{n} \rangle w_{nml}$, where $w_{nml} = \psi_1 - \psi_2$ is the width of the NML. Since NML is a region where the effect of turbulence spreading is significant, requiring $Ra \sim 1$ defines w_{nml} as

$$w_{nml} \sim \frac{2\pi}{\kappa \langle \tilde{v}\tilde{n} \rangle} \left(\frac{h\Delta x \Delta y}{u_x \tau_v}\right)^2 \frac{1}{v_* \tau_v^2} \frac{\Delta y}{a} \frac{\tau_v}{\tau_w}. \tag{14}$$

Obviously, w_{nml} depends on the void magnitude, void size, and waiting time (N.B., u_x and τ_v are also functions of h and Δx [9]). These parameters for voids can be further related to the amplitude, spatial scale, and frequency of GREs. The fact that w_{nml} is positively correlated with h and negatively correlated with τ_w implies that the stronger and more frequent the GREs, the wider the NML. To get a better sense of how big w_{nml} is, a specific set of parameters is adopted for an estimate. When $a \sim 10^3$, $\Delta x \sim \Delta y \sim 10$, $\tau_w \sim \tau_v \sim 10^3$, $v_* \sim u_x \sim 10^{-2}$, $\tilde{v} \sim \tilde{n} \sim 10^{-2}$, $\kappa/2\pi \sim 10^{-4}$, $h \sim 0.1$, we can see $w_{nml}/\rho_s \sim \mathcal{O}(10^2)$, which is quite sensible.

3.2. Comparison of shearing rate of void-driven flow to ambient shear

Following the aforementioned procedure, the ratios of the resulting shearing rate of void-driven flow ω_s^v to the ambient shear ω_s^a in these three cases are also calculated and summarized by Table 1. For $h \in (0.1,1)$, it can be

seen that ω_s^v could be comparable to ω_s^a in all three cases, and can exceed it in case (2). This result could (qualitatively) explain the correlation between zonal flow power bursts and the detection of voids in experiments [17]. We should emphasize that, although we choose a specific set of parameters for order-of-magnitude estimates of both w_{nml} and ω_s^v/ω_s^a, the conclusions do not lose generality. In practice, the values of these parameters, of course, vary across different experiments and devices. Nevertheless, the flexibility in our choice of parameters indicates that sufficiently large w_{nml} and ω_s^v/ω_s^a should exist in a considerably large portion of the parameter space. See Appendix B for a brief sensitivity analysis of the quantitative results.

TABLE 1. The ratio of the shearing rate of the void-driven zonal flow to the ambient shear in all three cases. Here v_F^a and Δ_F^a are the characteristic speed and width of the ambient shear, respectively. For evaluations of ω_s^v/ω_s^a, we assume $v_F^a \sim 10^{-2}$ and $\Delta_F^a \sim 10$. See the evaluation of w_{nml} and column 3 of this table for the values of other parameters.

Case	ω_s^v/ω_s^a	Parameters
①	$\left(\frac{h\Delta x\Delta y}{v_* u_x \tau_v a}\right)^2 \frac{\Delta_F^a}{v_F^a/v_*} \sim 10h^2$	$v_*, u_x \sim 10^{-2},\ x \to 0,$ $y \sim 10^2, t \sim a/v_* \sim 10^5$
②	$\left(\frac{h\Delta x\Delta y}{v_* u_x \tau_v}\right)^2 \frac{2\ln(a/v_*)\,\Delta_F^a}{x^3 v_F^a/v_*} \sim (10h)^2$	$v_*, u_x \sim 10^{-2},\ x \sim 10^2,$ $y \to 0, t \sim a/v_* \sim 10^5$
③	$\frac{\pi}{2}\left(\frac{h\Delta x\Delta y}{v_* u_y \tau_v}\right)^2 \frac{x}{a^3}\frac{\Delta_F^a}{v_F^a/v_*} \sim h^2$	$v_*, 2u_y \sim 10^{-2},\ x \sim 10,$ $y \sim 10^2, t \sim a/v_* \sim 10^5$

3.3. Prediction of the void lifetime

At this point, we already know that voids can drive drift wave turbulence and zonal flow, and thus account for the formation of a turbulent layer. But to close the feedback loop of the edge dynamics, we need to complete the other half of the story: the effects of turbulence and zonal flow on voids. One intuitive conjecture is that turbulence and flow can smear or shear the void, hence constraining the void lifetime. This process can be formulated by a diffusion equation

$$\frac{\partial}{\partial t} n_v = D\nabla_\perp^2 n_v, \tag{15}$$

where D is the turbulence diffusivity. Due to the properties of the diffusion equation, the magnitude of a given void will gradually decay. A practical definition of the void lifetime is the time it takes for its magnitude to decay to half of its initial value, which yields

$$\tau_v = \frac{2\Delta x^2}{D}. \tag{16}$$

If we consider a purely diffusive model, i.e., in the absence of shear, the turbulent diffusivity scales as $D \sim \tilde{v} l_{mix}$, where the mixing length $l_{mix} = L_n \rho_*^\delta$ ($\rho_* = \rho_s/L_n$, and L_n is the characteristic length of the mean density gradient [30]. However, in the presence of ambient shear (with the same shearing rate ω_s^a as above) and assuming $\rho_* \sim 10^{-2}$, a new form of the diffusivity emerges. The ratio of D to Bohm diffusivity $D_B \sim c_s \rho_s$ in these two branches are (1)

$$D/D_B \simeq \rho_*^\delta, \tau_v \propto \rho_*^{-\delta} \tag{17}$$

in the purely diffusive regime ($Dk_\perp^2 > \omega_s^a$ or $\frac{1}{2} < \delta < 1$) and (2)

$$D/D_B \simeq \rho_*^{(1+2\delta)/4}, \tau_v \propto \rho_*^{-(1+2\delta)/4} \tag{18}$$

in the shearing dominant regime ($Dk_\perp^2 < \omega_s^a$ or $0 < \delta < \frac{1}{2}$).

Figure 4 plots the predicted void lifetime as a function of δ. As can be seen, the comprehensive model (red line), which includes the ambient shear, raises the lower limit of our prediction compared with the purely diffusive

model (blue line). For $\omega_{ci} \sim 10^8$ s^{-1}, the calculated void lifetime ranges from a few to $100\,\mu$s, which agrees well with experimental results on MAST (green shade) [17].

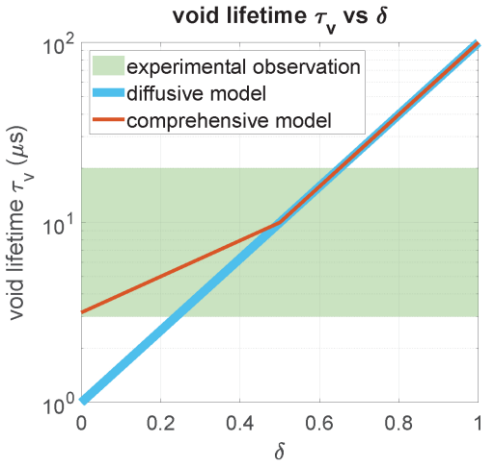

FIG. 4 Plot of the estimated void lifetime as a function of δ. *Here* $\delta = \ln(l_{mix}/L_n)/\ln(\rho_*)$ *is a dimensionless metric of the mixing length* l_{mix} *of the turbulence.*

4. CONCLUSION AND FUTURE PLAN

To summarize, by incorporating density voids into edge dynamics, we obtain quantitative estimates of the void-induced inward turbulence intensity flux, NML width, shearing rate of void-driven flow, and void lifetime. Once generated from GREs, voids can excite drift waves via Cherenkov emission, creating an edge-core coupling region of width $\sim 100\,\rho_s$, as derived from Eq. (14) for typical parameters. This picture explains the emergence of the shortfall in profile-driven gyrokinetic simulations, i.e., these suffer from the absence of GREs, void generation, and void-induced turbulence spreading. The fact that voids can drive zonal flow suggests a new mechanism of edge transport regulation. Under the effects of turbulence and zonal flow, the void lifetime is predicted to be between a few to $100\,\mu$s. Voids, drift waves, and zonal flow constitute a new feedback loop that goes well beyond the traditional drift wave–zonal flow paradigm [31,32]. We expect that our model applies not only to L-mode but also provides insights into H-mode, where GREs are present as edge-localized modes. For future research, we'd like to study the net effect of voids on edge transport. One key factor will be the ratio of the decorrelation time of the drift wave turbulence excited by voids to the shearing rate of void-driven zonal flow. In addition, we aim to consider the scattering of the void by the renormalized turbulent field to construct a fully self-consistent model. Since voids lose energy by emitting drift waves, this consideration may further restrain the upper limit of the predicted void lifetime. Furthermore, we also recommend looking for direct evidence of void–turbulence and/or void–zonal flow interactions in experiments by using wavelet bispectrum analysis.

ACKNOWLEDGEMENTS

We thank T. Long, A. Sladkomedova, and F. Khabanov for instructive and valuable discussion. This research was supported by the U.S. Department of Energy under Award No. DE-FG02-04ER54738. P. H. D. acknowledges support from LLNL-led SciDAC ABOUND Project SCW1832. The authors would like to thank the Isaac Newton Institute for Mathematical Sciences, Cambridge, for support and hospitality during the programme Anti-diffusive dynamics: from sub-cellular to astrophysical scales, where work on this paper was undertaken. This work was supported by EPSRC grant EP/R014604/1.

REFERENCES

[1] P. S. Marcus, Jupiter's great red spot and other vortices, Annu. Rev. Astron. Astrophys. 31 (1993) 523.
[2] J. A. Boedo et al., Transport by intermittent convection in the boundary of the DIII-D Tokamak, Phys. Plasmas 8 (2001) 4826.
[3] J. A. Boedo et al., Transport by intermittency in the boundary of the DIII-D Tokamak, Phys. Plasmas 10 (2003) 1670.
[4] T. H. Dupree, Growth of phase-space density holes, Phys. Fluids 26 (1983) 2460.

[5] Y. Kosuga, P. H. Diamond, Drift hole structure and dynamics with turbulence driven flows, Phys. Plasmas 19 (2012) 072307.
[6] A. Okubo, Horizontal dispersion of floatable particles in the vicinity of velocity singularities such as convergences, Deep Sea Res. Oceanogr. Abs. 17 (1970) 445.
[7] J. Weiss, The dynamics of enstrophy transfer in two-dimensional hydrodynamics, Physica D 48 (1991) 273.
[8] S. I. Krasheninnikov, D. A. D'Ippolito, J. R. Myra, Recent theoretical progress in understanding coherent structures in edge and SOL turbulence, J. Plasma Phys. 74 (2008) 679.
[9] D. A. D'Ippolito, J. R. Myra, S. J. Zweben, Convective transport by intermittent blob-filaments: Comparison of theory and experiment, Phys. Plasmas 18 (2011) 060501.
[10] S. Ding et al., A high-density and high-confinement Tokamak plasma regime for fusion energy, Nature 629 (2024) 555.
[11] C. Holland et al., Implementation and application of two synthetic diagnostics for validating simulations of core Tokamak turbulence, Phys. Plasmas 16 (2009) 052301.
[12] C. Holland, L. Schmitz, T. L. Rhodes, W. A. Peebles, J. C. Hillesheim et al., Advances in validating gyrokinetic turbulence models against L- and H-mode plasmas, Phys. Plasmas 18 (2011) 056113.
[13] B. B. Kadomtsev, Self-organization and transport in Tokamak plasma, Plasma Phys. Control. Fusion 34 (1992) 1931.
[14] T. S. Hahm, P. H. Diamond, Mesoscopic transport events and the breakdown of Fick's law for turbulent fluxes, J. Korean Phys. Soc. 73 (2018) 747.
[15] F. Khabanov et al., Density fluctuation statistics and turbulence spreading at the edge of L-mode plasmas, Nucl. Fusion 64 (2024) 126056.
[16] G. Dif-Pradalier et al., Transport barrier onset and edge turbulence shortfall in fusion plasmas, Commun. Phys. 5 (2022) 229.
[17] A. Sladkomedova, I. Cziegler, A. Field, A. Schekochihin, D. Dunai, P. Ivanov, Intermittency of density fluctuations and zonal-flow generation in MAST edge plasmas, J. Plasma Phys. 89 (2023) 905890614.
[18] A. Garg, Classical Electromagnetism in a Nutshell, Princeton University Press, Princeton, NJ (2012), Vol. 13.
[19] N. Rostoker, M. N. Rosenbluth, Test particles in a completely ionized plasma, Phys. Fluids 3 (1960) 1.
[20] T. Long et al., On how structures convey non-diffusive turbulence spreading, Nucl. Fusion 64 (2024) 064002.
[21] G. Xu et al., Blob/hole formation and zonal-flow generation in the edge plasma of the JET Tokamak, Nucl. Fusion 49 (2009) 092002.
[22] M. Wakatani, A. Hasegawa, A collisional drift wave description of plasma edge turbulence, Phys. Fluids 27 (1984) 611.
[23] O. E. Garcia, N. H. Bian, V. Naulin, A. H. Nielsen, J. J. Rasmussen, Mechanism and scaling for convection of isolated structures in nonuniformly magnetized plasmas, Phys. Plasmas 12 (2005) 090701.
[24] O. E. Garcia, N. H. Bian, W. Fundamenski, Radial interchange motions of plasma filaments, Phys. Plasmas 13 (2006) 082309.
[25] J. R. Myra, D. A. Russell, D. A. D'Ippolito, Collisionality and magnetic geometry effects on Tokamak edge turbulent transport. I. A two-region model with application to blobs, Phys. Plasmas 13 (2006) 112502.
[26] A. Hasegawa, K. Mima, Pseudo-three-dimensional turbulence in magnetized nonuniform plasma, Phys. Fluids 21 (1978) 87.
[27] P. H. Diamond, S.-I. Itoh, K. Itoh, Modern Plasma Physics, Cambridge University Press, Cambridge, England (2010).
[28] G. Veronis, On the transient response of a β-plane ocean, J. Oceanogr. Soc. Jpn. 14 (1958) 1.
[29] G. M. Webb, C. T. Duba, Q. Hu, Rossby wave Green's functions in an azimuthal wind, Geophys. Astrophys. Fluid Dyn. 110 (2016) 224.
[30] J. B. Taylor, B. McNamara, Plasma diffusion in two dimensions, Phys. Fluids 14 (1971) 1492.
[31] P. H. Diamond, Y.-M. Liang, B. A. Carreras, P. W. Terry, Self-regulating shear flow turbulence: A paradigm for the L to H transition, Phys. Rev. Lett. 72 (1994) 2565.
[32] P. H. Diamond, S.-I. Itoh, K. Itoh, T. S. Hahm, Zonal flows in plasma—a review, Plasma Phys. Control. Fusion 47 (2005) R35.